

ARTICLE

Received 27 Sep 2012 | Accepted 18 Jan 2013 | Published 19 Feb 2013

DOI: 10.1038/ncomms2521

OPEN

# Increased ventilation of Antarctic deep water during the warm mid-Pliocene

Zhongshi Zhang<sup>1,2,3</sup>, Kerim H. Nisancioglu<sup>1,2,4</sup> & Ulysses S. Ninnemann<sup>1,2,4</sup>

The mid-Pliocene warm period is a recent warm geological period that shares similarities with predictions of future climate. It is generally held the mid-Pliocene Atlantic Meridional Overturning Circulation must have been stronger, to explain a weak Atlantic meridional  $\delta^{13}\text{C}$  gradient and large northern high-latitude warming. However, climate models do not simulate such stronger Atlantic Meridional Overturning Circulation, when forced with mid-Pliocene boundary conditions. Proxy reconstructions allow for an alternative scenario that the weak  $\delta^{13}\text{C}$  gradient can be explained by increased ventilation and reduced stratification in the Southern Ocean. Here this alternative scenario is supported by simulations with the Norwegian Earth System Model (NorESM-L), which simulate an intensified and slightly poleward shifted wind field off Antarctica, giving enhanced ventilation and reduced stratification in the Southern Ocean. Our findings challenge the prevailing theory and show how increased Southern Ocean ventilation can reconcile existing model-data discrepancies about Atlantic Meridional Overturning Circulation while explaining fundamental ocean features.

<sup>1</sup>UNI Research, Allegaten 55, Bergen N-5007, Norway. <sup>2</sup>Bjerknes Centre for Climate Research, Allegaten 55, Bergen N-5007, Norway. <sup>3</sup>Nansen-Zhu International Research Center, Institute of Atmospheric Physics, Chinese Academy of Sciences, Beijing 100029, China. <sup>4</sup>Department of Earth Science, University of Bergen, Allegaten 41, Bergen N-5007, Norway. Correspondence and requests for materials should be addressed to Z.Z. (email: zhongshi.zhang@bjerknes.uib.no).

The mid-Pliocene warm period (mPWP, 3.264–3.025 Ma)<sup>1</sup> is known as the most recent period in the Earth's history when global average temperature was 2–3 °C warmer<sup>2–4</sup>, and estimations suggest global sea level was from 10 to 45 m (refs 5,6) above present level. These reconstructed warm temperatures of the mPWP are within the range of the Intergovernmental Panel on Climate Change projections of global temperature increases for the 21st century<sup>7</sup>. Furthermore, topography and bathymetry at the mid-Pliocene are similar to today. Thus, mPWP climate has frequently been discussed as an analogue for the long-term fate of the climate system, if the current levels of atmospheric greenhouse gas emissions are maintained<sup>2</sup>.

It is widely held that a stronger Atlantic Meridional Overturning Circulation (AMOC) with increased production of North Atlantic Deep Water (NADW) existed in the mPWP<sup>3,4,8,9</sup>, relative to the late Quaternary. Increased AMOC is thought to cause a weak meridional  $\delta^{13}\text{C}$  gradient in the Atlantic Ocean during the mPWP<sup>8–10</sup>, as well as a significant warming in the high latitudes of the North Atlantic<sup>3,4</sup>.

However, early climate models did not simulate a stronger AMOC when forced with Pliocene boundary conditions. Instead, coupled climate models forced with high atmospheric  $\text{CO}_2$  levels simulated a weaker AMOC<sup>11</sup>. More recent coupled climate model studies with improved mid-Pliocene boundary conditions from the Pliocene Research Interpretation and Synoptic Mapping (PRISM)<sup>3,4</sup> project still simulate a weak AMOC<sup>12,13</sup>. Although the model-data discrepancy in North Atlantic sea surface temperature (SST) is reduced in these simulations<sup>12,13</sup>, the model-data discrepancy in AMOC remains.

Here we further investigate the reason for the apparent mPWP model-data discrepancies. Using the  $\delta^{13}\text{C}$  compilation by Hodell and Venz<sup>10</sup> and the PRISM SST reconstructed by Dowsett *et al.*,<sup>3</sup> we begin by evaluating whether the two main observations argued to support the notion of a stronger AMOC during the mPWP—a

weak Atlantic meridional  $\delta^{13}\text{C}$  gradient and warming in the high-latitude North Atlantic—actually necessitate increased AMOC. We then compare available proxy data with a new mid-Pliocene experiment (see Method and Supplementary Methods) carried out with a state-of-the-art earth system model, the low-resolution version of the Norwegian Earth System Model (NorESM-L)<sup>14</sup>.

## Results

### The weak Atlantic meridional $\delta^{13}\text{C}$ gradient in the mPWP.

One possibility for reconciling the weak mPWP meridional  $\delta^{13}\text{C}$  gradient in the Atlantic<sup>8–10</sup> (Fig. 1a) with simulations of a reduced AMOC<sup>12,13</sup> is that the import of relatively young (high  $\delta^{13}\text{C}$ ) northern source deep water (NSW, for example, NADW) increased, despite little change in total overturning. Although this explanation is commonly invoked in paleoceanographic literature<sup>3,4,8,9</sup>, it is still at odds with existing data and simulations. Proxy evidence suggests that the physical property gradients (benthic foraminiferal  $\delta^{18}\text{O}$ ) between deep waters in the North (Deep Sea Drilling Project (DSDP) Site 607) and South Atlantic/Southern Ocean (Ocean Drilling Program (ODP) Site 1090/704) were maintained or even increased in the mPWP<sup>10</sup> (Fig. 1b). The increased deep water density (benthic  $\delta^{18}\text{O}$ ) gradient between the North and South Atlantic/Southern Ocean is at odds with the idea that a common water mass influences both of these regions. Furthermore, the large increases in Southern Ocean/South Atlantic  $\delta^{13}\text{C}$  do not occur at mid-depths<sup>10</sup> (ODP Site 1088, where NADW enters the Southern Ocean) where changes in NADW flux should have the largest effects<sup>15</sup>. Instead, the largest changes occur deeper, at depths occupied by southern source water (SSW)<sup>10,16</sup>. Existing mid-Pliocene simulations<sup>12,13</sup> appear consistent with this picture and do not show an increased export of deep water to the Southern Ocean/South Atlantic (south of 30°S).

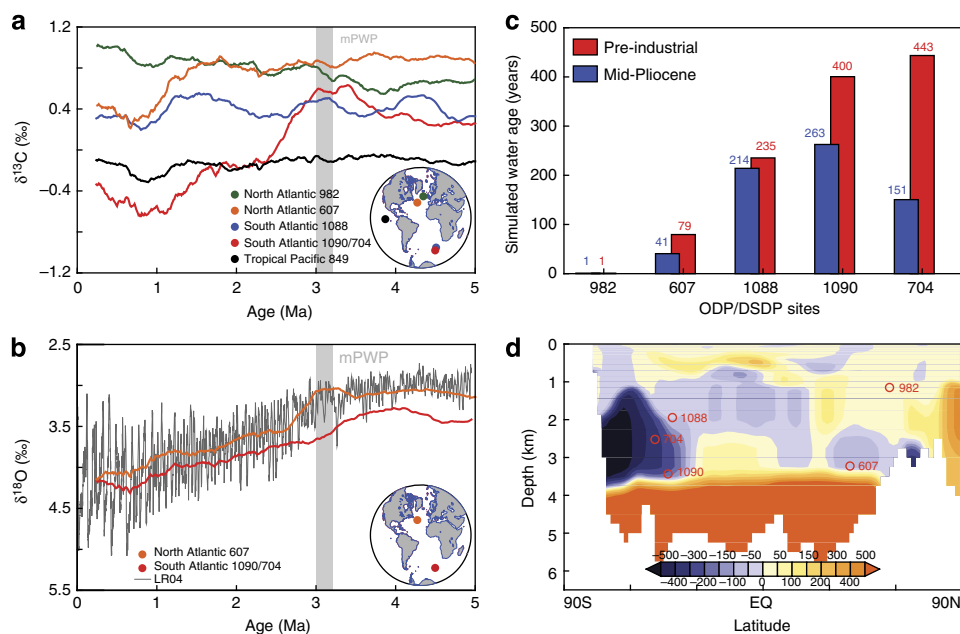


**Figure 1 | Benthic foraminiferal  $\delta^{13}\text{C}$  with comparison to simulated sea water ages.** (a) Compiled and smoothed benthic foraminiferal  $\delta^{13}\text{C}$  records in the Atlantic by Hodell and Venz<sup>10</sup>, according to the  $\delta^{13}\text{C}$  records from ODP Sites 982 (refs 10, 16, 19), 1088 (ref. 10), 1090/704 (refs 10, 16), 849 (ref. 21) and DSDP Site 607 (refs 10, 20). The  $\delta^{13}\text{C}$  data of Site 982 between 5 and 3 Ma are unpublished data from Raymo, but firstly appear in Hodell and Venz<sup>10</sup>. (b) Smoothed benthic foraminiferal  $\delta^{18}\text{O}$  records<sup>10</sup> at Site 607 and Site 1090/704, plotted against the LR04 benthic  $\delta^{18}\text{O}$  stack<sup>33</sup>. Site 1090/704 shows the composited data from Sites 1090 and 704 (ref. 10). For the mPWP, only Site 704 includes  $\delta^{13}\text{C}$  and  $\delta^{18}\text{O}$ . (c) Sea water ages (years) simulated at Sites 982, 607, 1088, 1090 and 704, red for the pre-industrial, and blue for the mid-Pliocene experiment. The numbers show the ages (years). (d) Age anomalies of Atlantic sea water (years). Sites 982, 607, 1088, 1090 and 704 are plotted according to latitude and depth.

Hence, we propose an alternative explanation that increased ventilation by SSW, rather than NSW, drives the observed changes in mPWP  $\delta^{13}\text{C}$ . A number of lines of evidence support enhanced ventilation and a weakly stratified<sup>17,18</sup> Southern Ocean/South Atlantic during the warm low-sea conditions of the mPWP relative to the late Quaternary. Hodell and Venz<sup>10</sup> argued that the large mPWP  $\delta^{13}\text{C}$  increase at deep Southern Ocean/South Atlantic Site 1090/704, and decreased Atlantic meridional  $\delta^{13}\text{C}$  gradient, could have been driven by increased input of high  $\delta^{13}\text{C}$  (young) SSW. In addition, they found a low vertical  $\delta^{13}\text{C}$  gradient, consistent with a weak vertical stratification<sup>17,18</sup> and increased deep ventilation in the Southern Ocean/South Atlantic during the mPWP. Together with the increased ventilation, the reduced sea ice cover<sup>17,18</sup> during the mPWP would have enhanced gas exchange and nutrient utilization relative to the late Quaternary, raising the preformed  $\delta^{13}\text{C}$  in deep water source regions<sup>10</sup>. Indeed, the  $\delta^{13}\text{C}$  of the deep Southern Ocean/South Atlantic<sup>10,16</sup> changes much more than North Atlantic<sup>10,16,19,20</sup> or Pacific<sup>21</sup> deep water values, also consistent with deep water changes that originate in the Southern Ocean.

Seen in this way, the low meridional  $\delta^{13}\text{C}$  gradient in the Atlantic is not evidence for a stronger mPWP AMOC. Rather, it is mainly caused by the high  $\delta^{13}\text{C}$  values from the well-ventilated and weakly stratified Southern Ocean/South Atlantic. As ventilation is reduced following the mPWP, a fundamental mode change in deep water formation occurs leading to the development of vertical<sup>10</sup> and interbasinal<sup>22</sup> gradients in Southern Ocean deep water properties.

To further test the hypothesis of a well-ventilated and weakly stratified mPWP Southern Ocean/South Atlantic, we compare the benthic foraminifera  $\delta^{13}\text{C}$  with the simulated water age in our experiments, as there is a good relationship between  $\delta^{13}\text{C}$  and water mass age in the ocean<sup>23</sup>. In the NorESM-L, an ideal age tracer is included to calculate water age—the time elapsed since a water parcel is in direct contact with the sea surface.

Changes in simulated water ages closely mimic the excursion trend of benthic foraminifera  $\delta^{13}\text{C}$  changes in the Atlantic since the mPWP (Fig. 1). In the mPWP there is little change in either measured  $\delta^{13}\text{C}$  or simulated ages at intermediate ocean depths (ODP Site 982) (refs 10, 16, 19) of the North Atlantic. In regions where NADW is prominent today, such as the deep North Atlantic (Site 607) and mid-depth Southern Ocean (Site 1088),  $\delta^{13}\text{C}$  values show a weakly negative excursion trend since the mPWP<sup>10,20</sup>, corresponding to simulated water ages being slightly younger in the mid-Pliocene experiment. By contrast to the relatively small changes in North Atlantic and intermediate ocean, deep water  $\delta^{13}\text{C}$  values in the Southern Ocean/South Atlantic (Site 1090/704) show a significant trend towards lower values since the mPWP<sup>10,16</sup>. Consistent with this, simulated water ages are significantly younger at these sites in our mid-Pliocene experiment. Thus, both the  $\delta^{13}\text{C}$  data and our simulations show that the largest changes in the mPWP occur in the deep Southern Ocean/South Atlantic.

The consistency between changes in deep water  $\delta^{13}\text{C}$  (in proxy records) and water mass age (in the simulations) is not surprising. The  $\delta^{13}\text{C}_{\text{DIC}}$  in the modern deep ocean is well correlated with water mass age<sup>23</sup> (Supplementary information) because newly formed (young) low-nutrient deep water has high  $\delta^{13}\text{C}$  values, which decrease with age due to mixing and the gradual respiration of low  $\delta^{13}\text{C}$  organic matter. What is more surprising is that this model-data consistency, in particular, the large decrease in Southern Ocean deep water ages, is accomplished without a significantly intensified AMOC. In our simulations, although the maximum overturning stream function is slightly larger in the mid-Pliocene experiment (23.4 Sv versus 21.8 Sv), the AMOC cell becomes shallower (Fig. 2a). Thus,

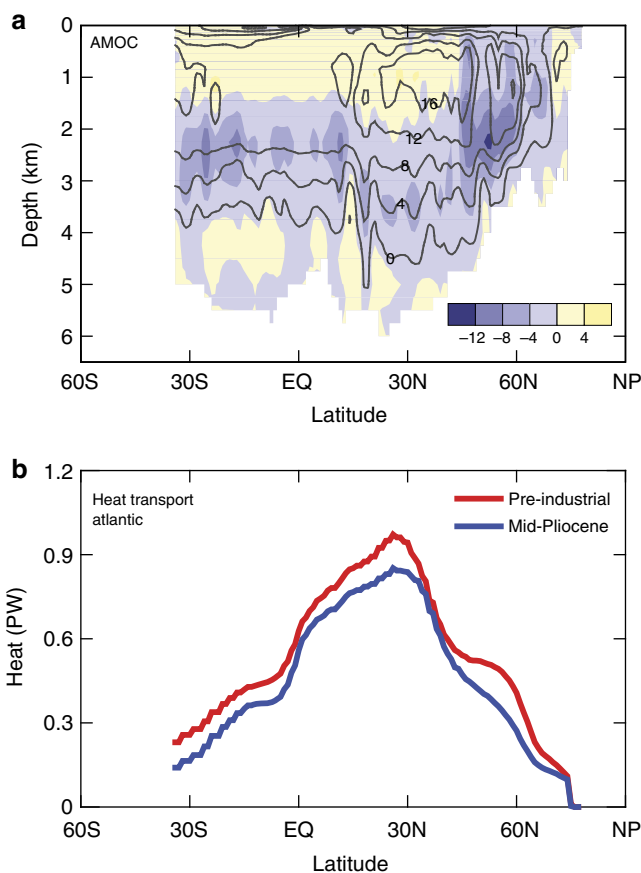


**Figure 2 | Simulated AMOC and ocean heat transport in the Atlantic.**

(a) Overturning stream function (Sv) simulated in the pre-industrial experiment (grey contours) and the difference between the mid-Pliocene experiment and the pre-industrial experiment (shaded areas). (b) Atlantic ocean northward heat transport (PW) simulated in the mid-Pliocene (blue) and the pre-industrial experiment (red).

despite a decrease and shoaling of Atlantic overturning, there is an increased amount of young water in the deep part of the Southern Ocean/South Atlantic in the mid-Pliocene experiment.

Our simulations are consistent with an increased role for the Southern Ocean/South Atlantic in deep ocean ventilation during the mPWP. The low vertical temperature and salinity gradients (weak stratification, Supplementary Figs S6 and S7) in the mid-Pliocene experiment, agree with proxy reconstructions showing a weakly stratified Southern Ocean/South Atlantic in the mid-Pliocene<sup>17,18</sup>. Accompanying the weak stratification, ventilation is intensified in the Southern Ocean/South Atlantic (Fig. 3). In the mid-Pliocene experiment, due to the smaller Antarctic ice-sheet<sup>24</sup> (though the extent of the ice-sheet is debated<sup>5,6,24</sup>), sea level pressure along the coast of Antarctica decreases and the wind stress strengthens and shifts poleward over the Southern Ocean/South Atlantic. As a result, easterlies along the coast of Antarctica strengthen as well as westerlies over the Antarctic Circumpolar Current (ACC) region (Supplementary Fig. S1). The importance of wind stress in ventilating the Southern Ocean is well documented<sup>25,26</sup>. In our mid-Pliocene simulation the strengthened easterlies drive increased Ekman convergence along the coast of Antarctica. Together with a significantly reduced mPWP sea ice cover in the mid-Pliocene experiment (Supplementary Fig. S2), the increased Ekman convergence causes enhanced downwelling of well-ventilated and relatively young surface water along the coast of Antarctica and into the deeper parts of the Southern

Ocean/South Atlantic (Supplementary Figs S3–S5). The efficient renewal of deep water (~2–4 km) in the mid-Pliocene experiment (relative to the pre-industrial) is consistent with the increased input of relatively young and high  $\delta^{13}\text{C}$  waters to the deep Southern Ocean/South Atlantic during the mPWP<sup>10</sup>.

**The warming in the high-latitude North Atlantic.** Other evidence used to support an intensified AMOC and stronger northward ocean heat transport in the mPWP is the reconstructed high SST in the northern high latitudes<sup>3,4,8</sup>. The PRISM3 reconstruction<sup>3</sup> shows that the SST in the central part of the high-latitude North Atlantic increases by 7 °C in February, and by 10 °C in August in the mPWP, relative to modern. Such warming is also demonstrated by other SST reconstructions<sup>27,28</sup> independent to PRISM3. In our mid-Pliocene experiment, the simulated warming is equivalent in scale to the SST changes reconstructed by PRISM3 in the Atlantic (Fig. 4a). In the high-latitude North Atlantic, annual mean SST increases by 7 °C. The simulated spatial pattern of warming is shifted compared with the reconstructions for the North Atlantic (Fig. 4b). This spatial discrepancy could be due to uncertainties in the proxy reconstructions, or changes in the simulated surface ocean circulation. Considering the potential uncertainties in the reconstructions, our simulations agree reasonably with the PRISM3 reconstructions on drilling sites in the North Atlantic. Although the scale of our simulated North Atlantic warming is as large as in the proxy reconstructions, the total northward ocean heat transport in the Atlantic is reduced (Fig. 2b). Therefore, the simulated warm surface temperatures at high latitudes of the North Atlantic cannot be simply attributed to changes in meridional overturning and heat transport by the ocean.

Seen in this way, observations of strong high-latitude warming are not sufficient to constrain the strength of the AMOC. Our simulation provides a clear example of a strong surface warming in the North Atlantic without intensified northward ocean heat transport. More likely candidates<sup>29</sup> to account for the observed amplification of warming at high latitudes in the mPWP are the direct radiative effect of increased greenhouse gas levels, and a significant decrease in the size and topography of the Greenland ice sheet.

**Discussion**

Our study demonstrates that neither an increase in AMOC nor in the export of NSW to the Southern Ocean is necessary to explain

the weak mPWP  $\delta^{13}\text{C}$  gradient. Instead, we suggest that mPWP deep ocean  $\delta^{13}\text{C}$  changes are driven mainly by increased preformed  $\delta^{13}\text{C}$  values in the deep waters originating in the well-ventilated and weakly stratified Southern Ocean. In our simulations, the increased ventilation in the mPWP Southern Ocean/South Atlantic is maintained by a strengthening of the zonal wind stress over the Southern Ocean and an increase of Ekman convergence near Antarctica. Furthermore, our mid-Pliocene simulation also provides a counter example, demonstrating that increased AMOC and intensified northward ocean heat transport by overturning are unnecessary to explain the magnitude of reconstructed high-latitude North Atlantic warming<sup>3</sup>. Thus, our simulations successfully explain the two main observations used to argue for an increased AMOC—but without increased AMOC.

Our experiments offer new insights into fundamental changes between mPWP and late Quaternary climate, which are testable with further proxy and modelling studies. In particular, the model

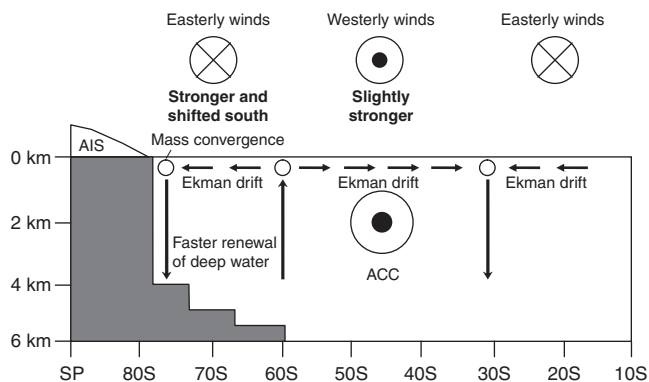


**Figure 3 | Southern Ocean/South Atlantic dynamics during the mPWP.** The schematic figure illustrates simulated changes in zonal mean surface winds as well as the wind-driven ocean circulation in the mid-Pliocene experiment. The position of ACC and winds represents the mean situation of the ocean dynamics in the mid-Pliocene. The bold texts show the changes between the mid-Pliocene and the pre-industrial.

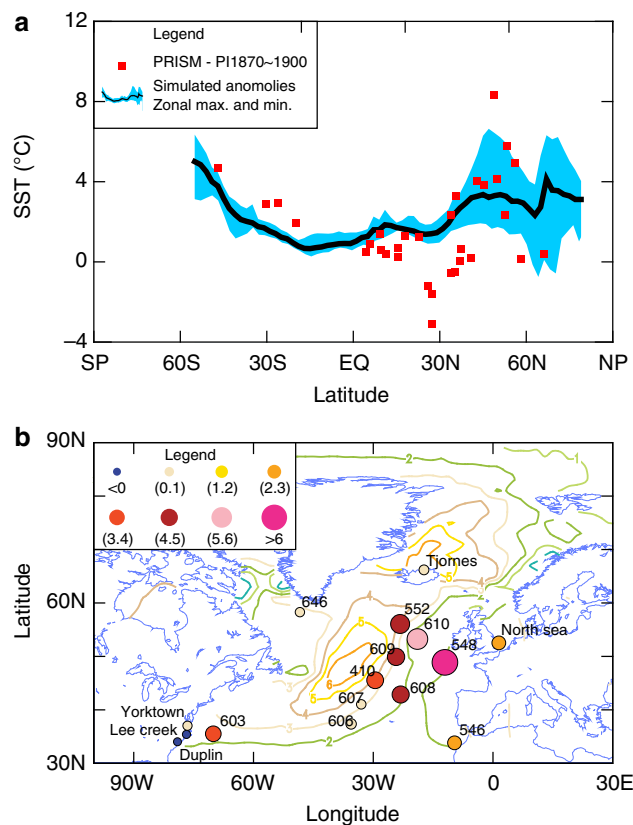


**Figure 4 | Comparison between PRISM and simulated Atlantic SST.** (a) Simulated zonal mean annual Atlantic SST anomalies (°C) between the mid-Pliocene and the pre-industrial experiment, compared with SST anomalies at ocean drilling sites between PRISM Pliocene SST reconstructed by Dowsett *et al.*<sup>3</sup> and 1870–1900 HadiSST<sup>34</sup>. The bold black line is the simulated zonal mean anomaly, and the blue area shows the maximum (max.) and minimum (min.) zonal anomalies. (b) Simulated annual mean SST anomalies, compared with reconstructed annual mean SST anomalies (circles) from available PRISM3 sites<sup>3</sup> in the North Atlantic. The reconstructed annual mean anomalies are the average of February and August PRISM3 values. PRISM3 includes reconstruction for 40 sites in the Atlantic. In these 40 sites, 32 sites have both February and August temperature estimates. Reconstructions without both February and August temperature estimates in the PRISM3 SST data set are not used here. Thus, in the North Atlantic map (b), ODP Sites 907, 909 and 911 are not included.

dependency of the response to Southern Ocean wind stress changes should be assessed, as well as the impact of different orbital forcing, ocean bathymetry and Antarctic ice sheet configurations. Along these lines, more Pliocene time slices or transient modelling could be used to determine whether the increased ventilation mode is unique to the mPWP or applies more generally to the Pliocene Southern Ocean/South Atlantic—how should the deep ventilation vary with evolving surface properties and sea ice in the Southern Ocean/South Atlantic portrayed by proxy data. Finally, as the deep water density (benthic  $\delta^{18}\text{O}$ ) gradient was more prominent during the mid-Pliocene (Fig. 1b), proxy constraints on deep water physical properties (temperature and salinity) could be crucial for model-data comparisons, elucidating the various sources and formation processes of Pliocene deep water.

Our results also highlight the widespread impact of Southern Ocean warming and associated sea ice retreat on the global ocean during the mPWP. For example, increased ventilation and reduced stratification in the Southern Ocean/South Atlantic could help explain high atmospheric  $\text{CO}_2$  levels in the mPWP, by allowing greater venting of  $\text{CO}_2$  from the deep ocean<sup>10,17</sup>. In our experiments, high atmospheric  $\text{CO}_2$  levels played a more important role than ocean heat transport and AMOC in accounting for the high-latitude warming during the mPWP. Likewise, our simulations agree well with the productivity indicators<sup>17,18</sup> and the changes in the intermediate-to-deep  $\delta^{13}\text{C}$  gradient<sup>10</sup>, which demonstrate that a major shift in Southern Ocean stratification happened since the mPWP. Finally, mid-Pliocene changes in global ocean productivity, upwelling and nutrient cycling pathways<sup>30</sup> have all been linked to Southern Ocean circulation changes. Taken together, our results suggest that increased Southern Ocean ventilation can explain many of the differences in the mid-Pliocene ocean, and may be an important harbinger for understanding the consequences of a warmer ocean.

## Method

**Experimental setup.** The mid-Pliocene experiment and the pre-industrial control experiment presented in this study are configured following the Pliocene Model Intercomparison Project (PlioMIP) experimental guidelines<sup>24</sup>. The mid-Pliocene experiment represents the peak warm period (3.264–3.025 Ma) (ref. 1) in the mid-Pliocene.

In the experiments, atmospheric  $\text{CO}_2$  levels are set to 405 ppmv for the mid-Pliocene, and 280 ppmv for the pre-industrial. The mid-Pliocene topography and vegetation conditions<sup>4</sup> reconstructed by the PRISM project are used as boundary conditions in the mid-Pliocene experiment. The pre-industrial and the mid-Pliocene experiment are initialized with identical initial temperature and salinity, and integrated for 1,500 model years. The simulated sea water ages indicate the 1,500-year integrations are long enough for the Atlantic section to reach equilibrium in the pre-industrial and the mid-Pliocene experiment. More details about the model and boundary conditions have been described in the references 14,31,32 and also in the Supplementary Methods of this article.

## References

- Dowsett, H. J. *et al.* An assessment of confidence in Pliocene global sea-surface temperature. *Nat. Clim. Change* **2**, 365–371 (2012).
- Jansen, E. *et al.* Palaeoclimate. In *Climate Change 2007: The Physical Science Basis, Contribution of Working Group I to the Fourth Assessment Report of the Intergovernmental Panel on Climate Change*. (eds Solomon, S. *et al.*) 433–497 (Cambridge Univ. Press, 2007).
- Dowsett, H. J., Robinson, M. M. & Foley, K. M. Pliocene three-dimensional global ocean temperature reconstruction. *Clim. Past* **5**, 769–783 (2009).
- Dowsett, H. J. *et al.* The PRISM3D paleoenvironmental reconstruction. *Stratigraphy* **7**, 123–139 (2010).
- Raymo, M. E., Mitrova, J. X., O'Leary, M. J., DeConto, R. M. & Hearty, P. J. Departures from eustasy in Pliocene sea-level records. *Nat. Geosci.* **4**, 328–332 (2011).
- Miller, K. G. *et al.* High tide of the warm Pliocene: implications of global sea level for Antarctic deglaciation. *Geology* **40**, 407–410 (2012).
- Meehl, G. A. *et al.* Global climate projections. In *Climate Change 2007: The Physical Science Basis, Contribution of Working Group I to the Fourth Assessment Report of the Intergovernmental Panel on Climate Change*. (eds Solomon, S. *et al.*) 770–772 (Cambridge Univ. Press, 2007).
- Raymo, M. E., Grant, B., Horowitz, M. & Rau, G. H. Mid-Pliocene warmth: stronger greenhouse and stronger conveyor. *Mar. Micropaleontol.* **27**, 313–326 (1996).
- Ravelo, A. C. & Andreasen, D. H. Enhanced circulation during a warm period. *Geophys. Res. Lett.* **27**, 1001–1004 (2000).
- Hodell, D. A. & Venz-Curtis, K. A. Late Neogene history of deepwater ventilation in the Southern Ocean. *Geochem. Geophys. Geosyst.* **7**, Q09001 (2006).
- Manabe, S., Stouffer, R. J., Spelman, M. J. & Bryan, K. Transient response of a coupled ocean-atmosphere model to gradual changes of atmospheric  $\text{CO}_2$ , part I: annual mean response. *J. Climate* **4**, 785–818 (1991).
- Haywood, A. M. & Valdes, P. J. Modelling Middle Pliocene warmth: contribution of atmosphere, oceans and cryosphere. *Earth Planet. Sci. Lett.* **218**, 363–377 (2004).
- Yan, Q., Zhang, Z.-S., Wang, H.-J., Jiang, D.-B. & Zheng, W.-P. Simulation of sea surface temperature changes in the Middle Pliocene warm period and comparison with reconstructions. *Chinese Sci. Bull.* **56**, 890–899 (2011).
- Zhang, Z.-S. *et al.* Pre-industrial and mid-Pliocene simulations with NorESM-L. *Geosci. Model Dev.* **5**, 523–533 (2012).
- Rutberg, R. L. & Peacock, S. L. High-latitude forcing of interior ocean  $\delta^{13}\text{C}$ . *Paleoceanography* **21**, PA2012 (2006).
- Venz, K. A. & Hodell, D. A. New evidence for changes in Plio-Pleistocene deep water circulation from Southern Ocean ODP Leg 177 Site 1090. *Palaeogeogr. Palaeoclimatol. Palaeoecol.* **182**, 197–220 (2002).
- Sigman, D. M., Jaccard, S. A. & Haug, G. H. Polar ocean stratification in a cold climate. *Nature* **428**, 59–63 (2004).
- Hillenbrand, C. D. & Fütterer, D. K. Neogene to quaternary deposition of opal on the continental rise west of the Antarctic Peninsula, ODP Leg 178, Sites 1095, 1096 and 1101. *Proc. Ocean Drill. Program Sci. Res.* **178**, 1–33 (2001).
- Venz, K. A., Hodell, D. A., Stanton, C. & Warnke, D. A 1.0 Myr record of glacial North Atlantic Intermediate water variability from ODP site 982 in the northeast Atlantic. *Paleoceanography* **14**, 42–52 (1999).
- Raymo, M. E., Hodell, D. A. & Jansen, E. Response of deepwater circulation to initiation of Northern Hemisphere glaciation (3–2 Ma). *Paleoceanography* **7**, 645–672 (1992).
- Mix, A. C. *et al.* Benthic foraminifer stable isotope record from site 849 (0–5 Ma): local and global climate changes. *Proc. Ocean Drill. Program Sci. Res.* **138**, 371–412 (1995).
- Waddell, L. M., Hendy, I. L., Moore, T. C. & Lyle, M. W. Ventilation of the abyssal Southern Ocean during the late Neogene: a new perspective from the subantarctic Pacific. *Paleoceanography* **24**, PA3206 (2009).
- Rohling, E. & Cooke, S. Stable oxygen and carbon isotopes in foraminiferal carbonate shells. In *Modern Foraminifera*. (eds Sen Gupta, B. K.) 239–258 (Kluwer Academic, 1999).
- Haywood, A. M. *et al.* Pliocene Model Intercomparison Project (PlioMIP): experimental design and boundary conditions (experiment 2). *Geosci. Model Dev.* **4**, 571–577 (2011).
- Oke, P. R. & England, M. H. Oceanic response to changes in the latitude of the Southern Hemisphere subpolar westerly winds. *J. Climate* **17**, 1040–1054 (2004).
- Russell, J. L., Dixon, K. W., Gnanadesikan, A., Stouffer, R. & Toggweiler, J. R. The Southern Hemisphere westerlies in a warming world: propping open the door to the deep ocean. *J. Climate* **19**, 6382–6390 (2006).
- Naafs, D. A. *et al.* Strengthening of North American dust sources during the late Pliocene (2.7 Ma). *Earth Planet. Sci. Lett.* **317–318**, 8–19 (2012).
- Lawrence, K. T., Sosdian, S., White, H. E. & Rosenthal, Y. North Atlantic climate evolution through the Plio-Pleistocene climate transitions. *Earth Planet. Sci. Lett.* **300**, 329–342 (2010).
- Lunt, D. J. *et al.* On the causes of mid-Pliocene warmth and polar amplification. *Earth Planet. Sci. Lett.* **321–322**, 128–138 (2012).
- Etourneau, J., Martinez, P., Blanz, T. & Schneider, R. Pliocene–Pleistocene variability of upwelling activity, productivity, and nutrient cycling in the Benguela region. *Geology* **37**, 871–874 (2009).
- Zhang, Z.-S. & Yan, Q. Pre-industrial and mid-Pliocene simulations with NorESM-L—AGCM simulations. *Geosci. Model Dev.* **5**, 1033–1043 (2012).
- Bentsen, M. *et al.* The Norwegian Earth System Model, NorESM1-M—part 1: description and basic evaluation. *Geosci. Model Dev. Discuss* **5**, 2843–2931 (2012).
- Lisiecki, L. E. & Raymo, M. E. A Pliocene–Pleistocene stack of 57 globally distributed benthic  $\delta^{18}\text{O}$  records. *Paleoceanography* **20**, PA1003 (2005).
- Rayner, N. A. *et al.* Global analyses of sea surface temperature, sea ice, and night marine air temperature since the late nineteenth century. *J. Geophys. Res.* **108**, 4407 (2003).

## Acknowledgements

We thank Bjorg Risebrobakken, Carin Andersson and Eystein Jansen for constructive comments to an early version of this paper. We also thank Mats Bentsen, Ingo Bethke, Jerry Tjiputra, Qing Yan for the discussions and for fruitful discussions and help in setting up and running the NorESM-L. This study was jointly supported by the National 973 Program of China (Grant No. 2010CB950102), the Strategic and Special Frontier Project of Science and Technology of the Chinese Academy of Sciences (Grant No. XDA05080803), the National Natural Science Foundation of China (Grant No. 40902054) and the Earth System Modelling (ESM) project financed by Statoil, Norway. All experiments carried out in this study were supported by the ESM project.

## Author contributions

Z.Z. developed the NorESM-L and carried out the simulations. Z.Z., K.N. and U.N. contributed to discussion of the results and writing of the manuscript.

## Additional information

**Supplementary Information** accompanies this paper at <http://www.nature.com/naturecommunications>

**Competing financial interests:** The authors declare no competing financial interests.

**Reprints and permission** information is available online at <http://npg.nature.com/reprintsandpermissions/>

**How to cite this article:** Zhang, Z.-S. *et al.* Increased ventilation of Antarctic deep water during the warm mid-Pliocene. *Nat. Commun.* 4:1499 doi: 10.1038/ncomms2521 (2013).



This work is licensed under a Creative Commons Attribution-NonCommercial-ShareAlike 3.0 Unported License. To view a copy of this license, visit <http://creativecommons.org/licenses/by-nc-sa/3.0/>